agronomy

MDPI

Article

Integrated Approaches for Adsorption and Incorporation Testing of Green-Synthesized TiO_2NPs Mediated by Seed-Priming Technology in *Punica granatum* L.

Hala M. Abdelmigid [1,*], Amal Ahmed Alyamani [1], Nahed Ahmed Hussien [2], Maissa M. Morsi [2] and Afnan Alhumaidi [1]

[1] Department of Biotechnology, College of Science, Taif University, P.O. Box 11099, Taif 21944, Saudi Arabia; a.yamani@tu.edu.sa (A.A.A.); afnan.m@tu.edu.sa (A.A.)
[2] Department of Biology, College of Science, Taif University, P.O. Box 11099, Taif 21944, Saudi Arabia; n.nahed@tu.edu.sa (N.A.H.); m.moasa@tu.edu.sa (M.M.M.)
* Correspondence: h.majed@tu.edu.sa

Abstract: Seed priming is a novel approach that is undertaken to improve seed germination and therefore potentially enhance growth and yield. Low-cost, eco-friendly, and efficient seed treatment as a means of enhancing growth and yield is still being sought for high-value crops such as pomegranates (*Punica granatum* L.), particularly in areas situated at high altitudes such as the Taif region. The uptake of nanoparticles (NPs) by plants provides a potential pathway for NP exposure. Therefore, it is imperative to understand NP uptake via seed priming and their unique properties within plants. In the present study, titanium dioxide nanoparticles (TiO_2NPs) were green-synthesized and utilized as priming agents for pomegranate seeds at a concentration of 40 mg/mL for 24 h. The adsorption of NPs was verified by scanning electron microscopy (SEM) and energy dispersive X-ray analysis/spectroscopy (EDX), while their incorporation was detected by transmission electron microscopy (TEM). To validate the EM results, X-ray fluorescence (XRF) and inductively coupled plasma optical emission spectroscopy (ICP–OES) techniques were further undertaken. The results confirmed the successful synthesis of pure anatase TiO_2NPs by employing aqueous extracts of pomegranate fruit peel (PPE) and coffee ground beans (CE). All of the analytical techniques employed in this research confirmed the incorporation of TiO_2NPs inside seeds, even after storage during priming treatment. This study lays the foundation for future sustainable seed technologies in terms of crop productivity and seed germination.

Keywords: TiO_2 nanoparticles; green synthesis; *Punica granatum* L.; seed priming

check for updates

Citation: Abdelmigid, H.M.; Alyamani, A.A.; Hussien, N.A.; Morsi, M.M.; Alhumaidi, A. Integrated Approaches for Adsorption and Incorporation Testing of Green-Synthesized TiO_2NPs Mediated by Seed-Priming Technology in *Punica granatum* L. *Agronomy* **2022**, *12*, 1601. https://doi.org/10.3390/agronomy12071601

Received: 11 May 2022
Accepted: 30 June 2022
Published: 2 July 2022

Publisher's Note: MDPI stays neutral with regard to jurisdictional claims in published maps and institutional affiliations.

Copyright: © 2022 by the authors. Licensee MDPI, Basel, Switzerland. This article is an open access article distributed under the terms and conditions of the Creative Commons Attribution (CC BY) license (https://creativecommons.org/licenses/by/4.0/).

1. Introduction

Plant seeds are the first link in the chain of agricultural production, and they provide the fundamentals for natural crop development. In this regard, seeds contain the genetic potential of variations and, consequently, play a significant role in determining the ultimate yield. Hence, seed production is an integral part of any food security strategy for any enterprise. Uniform seed germination is essential for ensuring high agricultural productivity and economic sustainability via the efficient use of production resources in commercial agriculture [1,2]. This is especially evident in high-value crops such as pomegranate (*Punica granatum* L.), where the demand and production of high-quality varieties are widespread. Moreover, the development of new cultivars relies on the ability of plant breeders to produce plants from seeds.

Many crop species have semipermeable layers in their seed coat for gas exchange, water uptake and solute leakage constraints. Most commercial pomegranate cultivars have hard or semihard seed coats that could affect water permeability and consequently seed germination [3]. This might further give rise to oxygen starvation, resulting in poor

germination, inconsistent emergence, and poor development [4]. For improving seed coat permeability to water and oxygen, a variety of strategies have been employed, including scarification, nicking, and removing the seed coat; however, these techniques exhibit variable levels of success. Therefore, novel seed technologies are necessary for improving seed germination and seedling vigor.

Seed priming is an innovative ecological seed technology to enhance seed vigor and crop production without compromising ecosystems. It provides an opportunity to improve the quality and yield of economic crops. Seed priming has been found to result in more vigorous seedling growth and faster establishment [5,6]. It also stimulates the activity of enzymes that break down macromolecules for the growth and development of the embryo and eventually results in higher rates of seedling emergence and flourishing its establishment [7]. These biological effects of priming would be beneficial to farmers since they would reduce the time and cost of reseeding and supplemental irrigation; however, a reduction in seed storage life and viability is the main disadvantage of priming and the principal constraint to its diffusion because dehydration to the initial moisture is needed before storage. This limitation can be addressed by identifying the genes/markers for determining the impact of priming on germination efficiency and seed vigor. Each priming technique, in some way, increases the productivity and yield but requires standardization due to several factors to be taken into consideration. Nanopriming is a new emerging seed technology that combines seed-priming science with nanotechnology to create smart agriculture [8,9]. It is believed that nanopriming might provide protection for seeds during storage and improve the germination, plant growth, and resistance of crops to abiotic or biotic stresses, thereby lowering pesticide and fertilizer requirements [10]. Recently, seed nanopriming has been proven to stimulate different genes during germination, especially those related to plant stress resistance [11–13].

The green synthesis of nanoparticles is an additional sophistication of nanotechnology to produce safe nanoscale biomaterials for agricultural applications. In the past decade, a series of reports have demonstrated that plant-based systems have significant advantages over other biological systems, which leads them to be preferred platforms for nanoparticle synthesis. Plant extract metabolites play an essential role in the bioreduction of inorganic metal ions into metal nanoparticles [14–16]. The current study is focused on the green synthesis of TiO_2NPs using two different plant extracts. Based on our previous work [17], aqueous extracts of pomegranate (*Punica granatum* L.) peel and dark roasted ground beans (*Coffea arabica* L.) have been proven to develop valuable nanomaterials that are eco-friendly and cost-effective for large-scale production.

Nanotechnology is anticipated to impact a wide spectrum of applications, and the incorporation of nanomaterials into commercial products is expected to grow in the next few years. One of the most abundant nanomaterials produced is TiO_2 nanoparticles (NPs), which have a wide range of commercial uses, including agrochemicals [18]. Therefore, to detect and evaluate the potential risks in food safety, basic information is needed about the interactions between TiO_2NPs and plants, and more robust analytical methods are required to quantify the uptake and translocation of TiO_2NPs into plants. The stepwise evaluation begins by examining the exerted effects of nanoparticles on plant seeds [19]. Both preferred and detrimental biological effects are generated by NPs as a result of adsorption, uptake, penetration, and accumulation in the targeted tissues [20–22].

In addition to increasing growth and production attributes, TiO_2 nanoparticles have several important effects on the morphological, biochemical, and physiological characteristics of crops. Many researchers have reported improved germination and better development of radicle and plumule in seedlings when treated with TiO_2NPs [19–22]. There is, however, a lack of literature covering the biological effects of seed priming by TiO_2 nanoparticles in *Punica granatum* L. and the analytical methods used in nanoparticle–plant/seed interactions in this important crop.

Based on the unique physical and chemical properties of green-synthesized nanoparticles and their potential as a delivery mechanism for biological systems, we hypothesized

that seed priming would enhance the growth parameters of pomegranate crops in the region of Taif. However, despite new studies on nanoparticle–plant interactions, there are limitations in the available analytical techniques and sample pretreatment methods for the evaluation of NP uptake within biological tissues [18]. Thus, in the present study, the adsorption and uptake of green-synthesized TiO_2NPs in nanoprimed pomegranate seeds were comprehensively evaluated using different analytical techniques. After the exposure period, the deposition of TiO_2NPs was evaluated using electron microscopy (EM) coupled with energy-dispersive X-ray spectroscopy (EDX) for the direct visualization of nanomaterials on the seed surface and the qualitative determination of their elemental compositions. Additionally, inductively coupled plasma–optical emission spectroscopy (ICP–OES) and XRF (X-ray fluorescence) techniques were used to detect the incorporated nanoparticles in *P. granatum* L. seeds. This research presents a pioneering study of nanopriming's effects on the uptake and internalization of *P. granatum* (Taify variety) using various analytical detection methods.

2. Materials and Methods

2.1. Chemicals and Plant Materials

Titanium dioxide (TiO_2), required for TiO_2NPs, was purchased from Acros Organics, Geel, Belgium. Pomegranate (*Punica granatum* L.) fruits and coffee beans were purchased from a local market in the Taif Governorate, KSA. The plant study was in compliance with relevant institutional, national, and international guidelines and legislation.

2.2. Preparation of Plant Extracts

This research was conducted in 2020 in the central laboratories at Taif University's deanship of scientific research. *P. granatum* L. fruits were washed thoroughly using distilled water and by separating the seeds from peels. The pomegranate peels were oven-dried at low temperatures overnight until completely dry, then ground into a coarse powder. The coffee beans were ground and dissolved in boiled water, and their waste was air-dried at room temperature. Pomegranate extracts (PPE) and coffee grounds (CE) were prepared according to a published protocol by Abdelmigid et al. [17].

2.3. Green Synthesis of TiO_2 Nanoparticles

For titanium dioxide nanoparticle (TiO_2NPs) biosynthesis, we followed the method of Swathi et al. [23] with minor modifications. First, 10 mL of each extract (PPE or CE) was separately mixed with 90 mL of aqueous 10^{-3} M TiO_2 solution. The mixture was heated in a water bath (60 °C) with continuous stirring until the color changed. Samples were centrifuged at 6000 rpm for 30 min, the supernatant was discarded, and pellets containing the synthesized TiO_2NPs were kept. Biosynthesized TiO_2NPs from PPE (TiO_2NPs_PPE) and CE (TiO_2NPs_CE) were dried overnight at 60 °C in glass Petri dishes, and finally, they were scraped out for further characterization and assessment [24].

2.4. Characterization of TiO_2 Nanoparticles

Bioreduction of Ti ions was determined in their aqueous form under ultraviolet–visible spectroscopy via optical absorption measurements. UV–Vis spectral analysis was conducted by a UV–Vis spectrophotometer (UV-1601, Shimadzu, Japan) in the typical range of 200–800 nm. The charge of the nanoparticle surfaces and their average size were measured by a particle size analyzer (Zetasizer Nano ZS, Malvern Instruments Ltd., Malvern, Worcestershire, UK). Similarly, the morphology and size of the TiO_2NPs were evaluated by transmission electron microscopy (TEM) at 100 kV. Using X-ray diffraction (XRD) analysis, the crystal structure and crystalline size of TiO_2NPs were confirmed using a powder X-ray diffractometer (PW3040/60 X'pertPRO, PANalytical, Noord-Holland, Netherlands). XRD was performed at 30 kV and 100 mA, and the spectrum was recorded by CuKα radiation with a wavelength of 1.5406 Å in the 2θ range of 20–80°. Patterns of XRD were plotted by software OriginLab. To determine the surface morphology of

biosynthesized TiO_2NPs, analytical scanning electron microscopy (SEM, JEOL JSM-639OLA, Tokyo, Japan) at 20 kV was used with different magnifications of X500, X2000, and X3000 with scale bars of 50 µm, 10 µm, and 5 µm, respectively. The functional groups of the PPE and CE extracts that are responsible for TiO_2NP formation and stabilization were confirmed using Fourier transform infrared (FTIR) spectrometry (Agilent Technologies, Santa Clara, CA, USA) in transmittance mode in the range of 450–4000 cm^{-1}.

2.5. Preparations of Nanopriming Solutions and Seed Priming

Two types of green-synthesized TiO_2NPs (40 mg/L) were freshly prepared by dispersing the prepared TiO_2NPs in Milli-Q deionized water using ultrasonic vibration (100 W, 40 kHz) for 30 min [11]. The concentration of the nanopriming solution was selected based on preliminary experiments. Seeds were surface sterilized in 1% sodium hypochlorite for 3 min and then rinsed with deionized water three times. Seeds were then soaked in TiO_2NP priming solutions for 24 h with continuous aeration (rotatory shaker). The ratio of seed weight to solution volume was 1:4 (gmL^{-1}). Seeds were rinsed with deionized water (3 min) and surface-dried on Whatman filter paper. Milli-Q deionized H_2O was defined as a hydropriming (HP) solution [11]. Seeds were dried back to their initial moisture content at room temperature, sealed in sterilized pouches, and stored at 4 °C until further use.

2.6. Assaying TiO_2NPs Adsorption on a Seed Surface by SEM Analysis

Nanoprimed seeds were washed with distilled water and then air-dried and examined by analytical scanning electron microscopy to evaluate the morphological characteristics and the distribution of the nanoparticles adsorbed on the surface of the seeds. Seeds were separately coated with gold using a Cressington 108 Sputter Coater (auto, thickness controller MTM-10, Watford, UK) for 10 min prior to scanning.

2.7. Energy Dispersive X-ray (EDX)

Dispersive spectrometry (EDX) was simultaneously applied for the chemical identification of the titanium dioxide nanoparticles and to identify the elemental percentage in the *P. granatum* L. seeds using a JEOL– JSM-1400 PLUS system with an EDX detector (JEOL, Tokyo, Japan. All samples were coated with a thin film of gold for analysis. In the EDX spectrum, the detected signal was plotted as a function of the (characteristic) energy.

2.8. Assaying TiO_2NPs Internalization by Transmission Electron Microscopy (TEM)

Randomly selected nanoprimed seeds were dissected and prefixed by immersing them at once in 4F1G in phosphate buffer solution (pH = 7.2) at 4 °C for 3 h. Specimens were then postfixed in 2% OsO_4 in the same buffer at 4 °C for 2 h. Samples were washed in buffer and dehydrated at 4 °C through a series of acetone concentrations. Subsequently, they were embedded in resin for polymerization and then cut into sections approximately 90 A in thickness. Sections were placed on grid copper, stained with uranyl acetate for 5 min, stained with 1% lead citrate for 2 min, rinsed again in pure water, and stored in a grid box. A Leica ultracut UCT ultramicrotome was used to prepare ultrathin sections. TEM images were obtained using a JEOL– JSM-1400 PLUS (JEOL, Tokyo, Japan) TEM at an accelerating voltage of 100 kV.

2.9. Inductively Coupled Plasma Spectrometer (ICP–OES) Analysis of NPs Uptake

For the measurement of total TiO_2NP uptake or bioaccumulation in nanoprimed pomegranate seeds, finely powdered seed samples (0.1 g) were dried at 100 °C for 24 h. Subsequently, they were digested with 10 mL aqua regia (HNO_3/HCL) and slowly heated at 150 °C until all residues were dissolved. This process was repeated twice with the addition of 10 mL aqua regia to obtain complete digestion (~2 mL). The solution was filtered through Whatman filter paper, transferred to a 100 mL volumetric flask, and diluted with Millipore water. Quantification of TiO_2NP content was performed in triplicate by using an inductively coupled plasma spectrometer (ICPE-9000, Shimadzu, Kyoto, Japan).

Before analysis, the instrument was calibrated with a standard blank and the mix-metal calibration standard. The analysis was started after obtaining the best linear regression correlation coefficient ($r^2 \geq 0.09999$) from the calibration plot. All analytical references and multielement standards were purchased from AccuStandard (New Haven, CT, USA).

2.10. Energy Dispersive X-ray Fluorescence (EDXRF) Analysis of NPs Uptake

This analysis was carried out following the protocol by Tezotto et al. [25]. The same pomegranate seed samples used for ICP–OES were used for EDXRF analysis and were prepared as loose powder. One gram of ground seeds was packed into a polyethylene cup of 20 mm internal diameter and covered with 6 µm-thick polypropylene film (Mylar®). The samples were irradiated in triplicate for 300 s under vacuum using a Shimadzu EDX-720 energy dispersive X-ray fluorescence spectrometer. The samples were irradiated using an Rh X-ray tube operated at 15 kV (Na to Sc) and 50 kV (Ti to U). The current was automatically adjusted (maximum of 1 mA). A 10 mm collimator was chosen. Detection was conducted using a Si (Li) detector cooled with liquid nitrogen. Certified reference materials (CRMs) were analyzed using the same method as described above to verify trueness and precision. The intensity of element Kα counts per second (cps/µA) was obtained from the sample X-ray spectrum deconvolution using the EDX Shimadzu software package.

3. Results

3.1. Titanium Dioxide Nanoparticles (TiO_2NPs) Characterization

3.1.1. UV–Vis Spectroscopy

The colors of plant extracts (PPE and CE) were changed to cloudy yellow or brown color after the addition of an aqueous white solution of TiO_2 and incubation, respectively (Figure 1A). The change in color is evidence of the successful formation of TiO_2NPs_PPE and TiO_2NPs_CE, as validated by UV–VIS spectroscopy. Figure 1B shows UV_Vis broad absorption spectra of TiO_2NPs_PPE at 350 nm and a sharp spectrum for TiO_2NPs_CE at 320 nm.

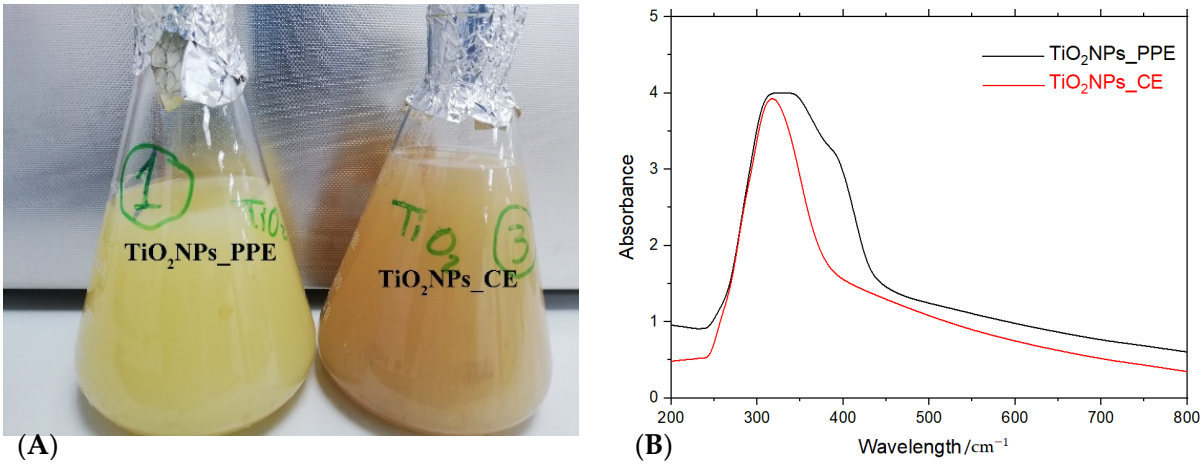


Figure 1. Green synthesis of titanium dioxide nanoparticles using pomegranate peel extract (PPE), and coffee ground extract (CE). (**A**). Change in color of the reaction to cloudy yellow and brown after the production of nanoparticles. (**B**). UV−Visible spectral analysis of green-synthesized titanium dioxide nanoparticles TiO_2NPs_PPE and TiO_2NPs_CE.

3.1.2. Scanning Electron Microscopy (SEM)

The SEM micrographs were examined at different magnifications of green-synthesized TiO_2NPs_PPE and TiO_2NPs_CE to reveal their surface morphology (Figure 2A). The SEM analyses showed that agglomerates of the nanoparticles were present in a randomly arranged manner with irregular sizes and shapes.

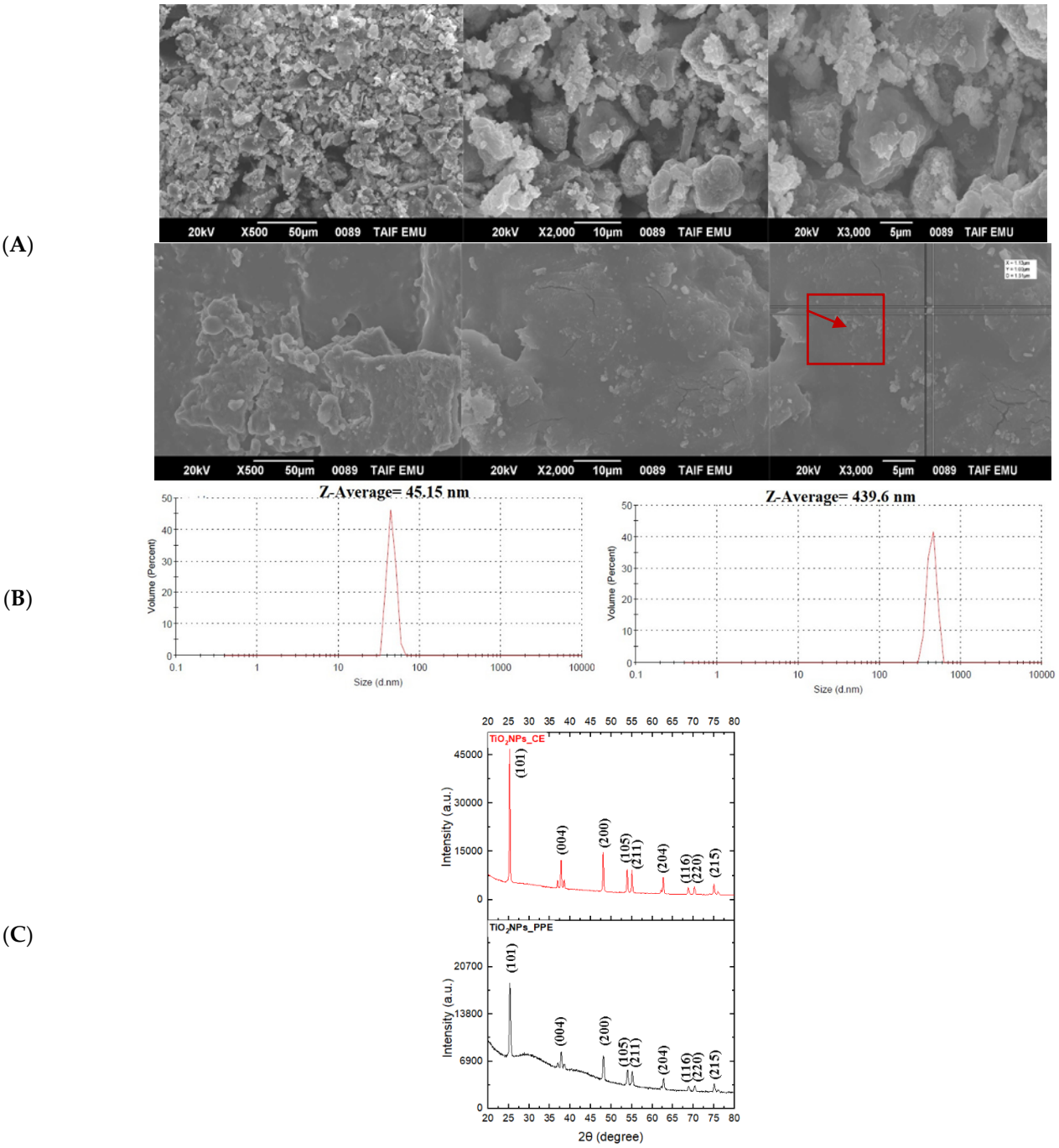


Figure 2. Size and shape properties of synthesized TiO_2NPs: (**A**) amorphous and crystalline shape showed by SEM image at different magnifications (Red box and arrow indicate the synthesized nanoparticles). (**B**) The average size revealed by Zeta potential analyzer and (**C**) anatase crystalline shape by XRD pattern, of TiO_2NPs_CE and TiO_2NPs_PPE.

3.1.3. Size Distribution and Zeta Potential

Figure 2B shows the mean size of the green-synthesized titanium dioxide nanoparticles TiO_2NPs_PPE (439.6 nm) and TiO_2NPs_CE (45.14 nm) with zeta potentials of −6.63 mV and −15.0 mV, respectively, by using the zeta sizer. However, the TEM images revealed different size measurements with mean values of (85.6 nm and 79.6 nm) for TiO_2NPs_PPE and TiO_2NPs_CE, respectively.

3.1.4. X-ray Diffraction

The XRD pattern of the synthesized TiO_2NPs also confirmed their crystalline nature. Both TiO_2NPs (PPE and CE) had the same XRD pattern that revealed six broad intense peaks in the whole spectrum of 2θ values. Figure 2C displays prominent diffraction peaks at 25.28°, 37.93°, 48.37°, 53.89°, 55.29°, and 62.73° indexed as the (101), (004), (200), (105), (211), and (204) according to JCPDS file No. 21-1272, respectively.

3.1.5. Fourier Transform Infrared Spectroscopy (FTIR)

To identify the main functional groups and chemical compounds found in the natural extracts (PPE and CE), which play a key role in the synthesis of TiO_2NPs, FTIR spectra of TiO_2NPs_PPE and TiO_2NPs_CE were recorded and compared with their PPE and CE extracts as references (Figure 3). A change in the sharpness or position of transmittance peaks between synthesized TiO_2NPs and their reference is referred to as a group contribution in the synthesis of TiO_2NPs. For TiO_2NPs_PPE, the functional group C–H is assigned to the band at approximately 1513–1516 cm^{-1}. The band at approximately 1269–1278 cm^{-1} refers to alcohol functional groups. The band assigned to 1057–1055 cm^{-1} corresponds to the aromatic C–O group vibration. The TiO_2NPs_CE spectra show more different sharp peaks and broad bands, in addition to those peaks that refer to flavonoids as in TiO_2NPs_PPE. The carbonyl C=O stretching vibration and the C=N stretching in the imidazole ring of caffeine appear at 1700 cm^{-1} and at 1403 cm^{-1}, respectively. Additionally, numerous vibrations of free caffeine appear at 2900, 1700, 1683, and 1456 cm^{-1}, and broad bands appear at 1284–973 and 925 cm^{-1}. Similarly, both green-synthesized TiO_2NPs exhibited strong bands at 460 cm^{-1} and 900 cm^{-1}, indicating the formation of Ti–O and Ti–O-Ti bending vibrations, respectively.

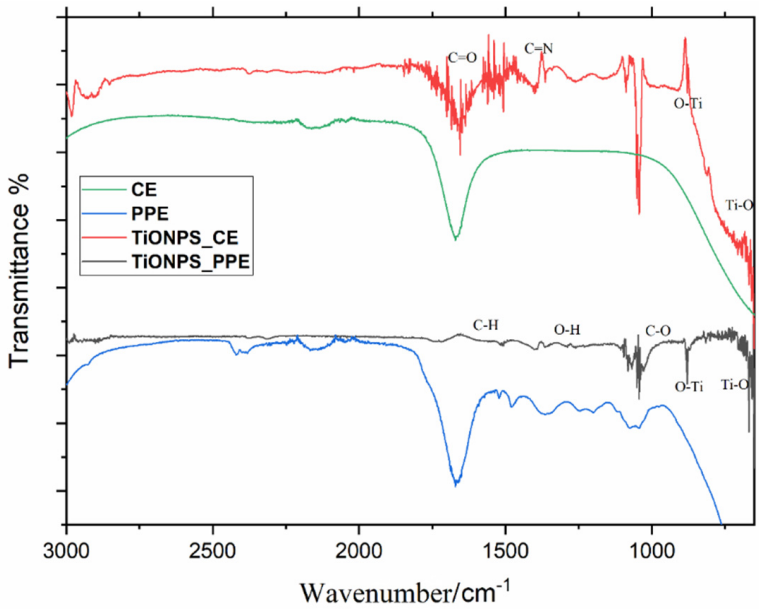


Figure 3. Comparative FTIR spectra of synthesized TiO_2NPs_PPE and TiO_2NPs_CE nanoparticles with their standards (PPE and CE).

3.2. TiO_2NP Adsorption and Localization on Seed Coats

SEM/EDX Analysis

Scanning electron microscopy (SEM) was applied to evaluate the features of the adsorbed TiO_2NPs' distribution on the surface of nanoprimed seeds. SEM was also applied to evaluate the morphology and integrity of the *P. granatum* seeds. Figure 4A–C show an SEM micrograph of TiO_2NPs_(PPE and CE)-nanoprimed *P. granatum* seeds in suspensions containing 40 mg/L compared to hydroprimed seeds. In general, the SEM results revealed the modification induced by NPs on the surface morphology of *P. granatum* seeds. Several large

pores with a honeycomb shape were observed on the surface of the TiO_2NP-nanoprimed seeds compared to the control seeds. Small and large aggregates of variable sizes were noticed on the seed surfaces in both treatments (TiO_2NPs_PPE and TiO_2NPs_CE) that were also trapped inside the fibers on the seed coat. A different pattern of cluster formation and distribution on the surface of the seeds was shown by each NP (Figure 4B,C). The formation of higher clusters was evident in TiO_2NPs_PPE on the surface of the seeds (Figure 4B). The TiO_2NPs_CE showed individual nanoparticles and some clusters. The TiO_2NPs in the cluster were loosely arranged, and individual nanoparticles could be easily recognized (Figure 4C), indicating that the clusters comprised agglomerates with weak binding forces.

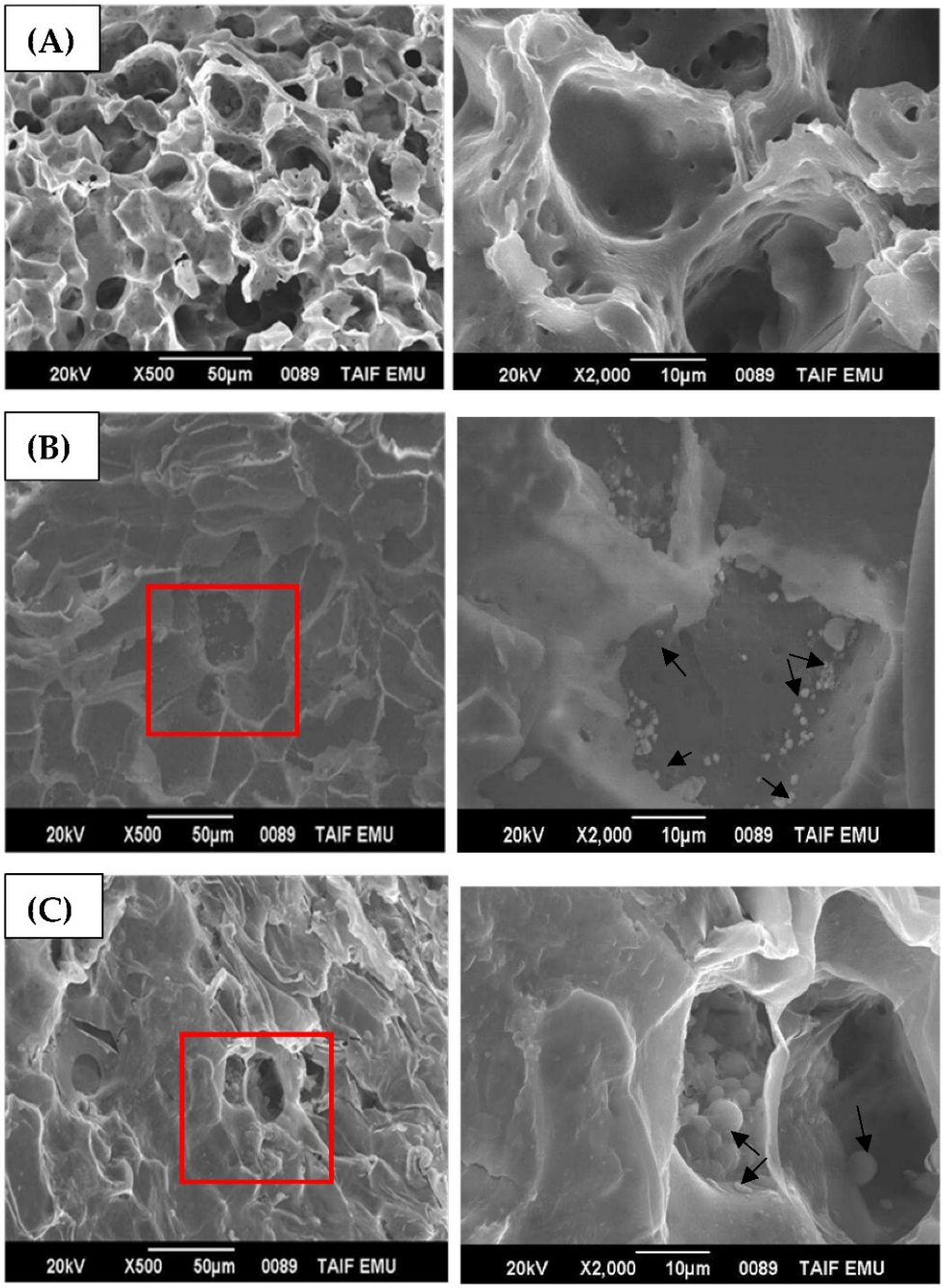


Figure 4. SEM micrographs of primed *P. granatum* seeds at different magnifications. (**A**) hydroprimed seeds; (**B**) TiO_2NPs_ PPE-primed seeds; and (**C**) TiO_2NPs_CE-primed seeds (red box and arrows show the adsorbed nanoparticles on seed coat surface).

Furthermore, EDX spectroscopy was simultaneously used for chemical identification/distribution of TiO_2NPs on the seed coat cellular structures, and the results confirmed the deposited TiO_2NPs on the seed coat surfaces. Conversely, the surface of the seeds in the hydroprimed (HP) samples was clear, and therefore no Ti signal was detected. The EDX spectra of TiO_2NPs are shown in Figure 5A–I, and the mass% of C, O and Ti elements is shown as bars. In comparison with the hydroprimed seeds, the EDX profile demonstrated the absorption of organic compounds (C and O) on the surface of NPs from the plant extracts of *P. granatum* (PPE) and *C. arabica* (CE), which were crucial for reducing and capping the TiO_2NPs. In contrast, the control seeds had a low mass percent of C (52.22%), whereas the O amount was high (47.78%) (Figure 5C). The analysis of the seed surface indicated variations between the amount of C and O within the nanoprimed samples. Evidently, TiO_2NPs_CE-primed seeds had the highest percent of carbon weight (69.36%) and the lowest amount of oxygen (26.49%) (Figure 5F), whereas TiO_2NP_PPE-nanoprimed seeds had a lower percent of C (60.15%) and more O (39.46%) (Figure 5I).

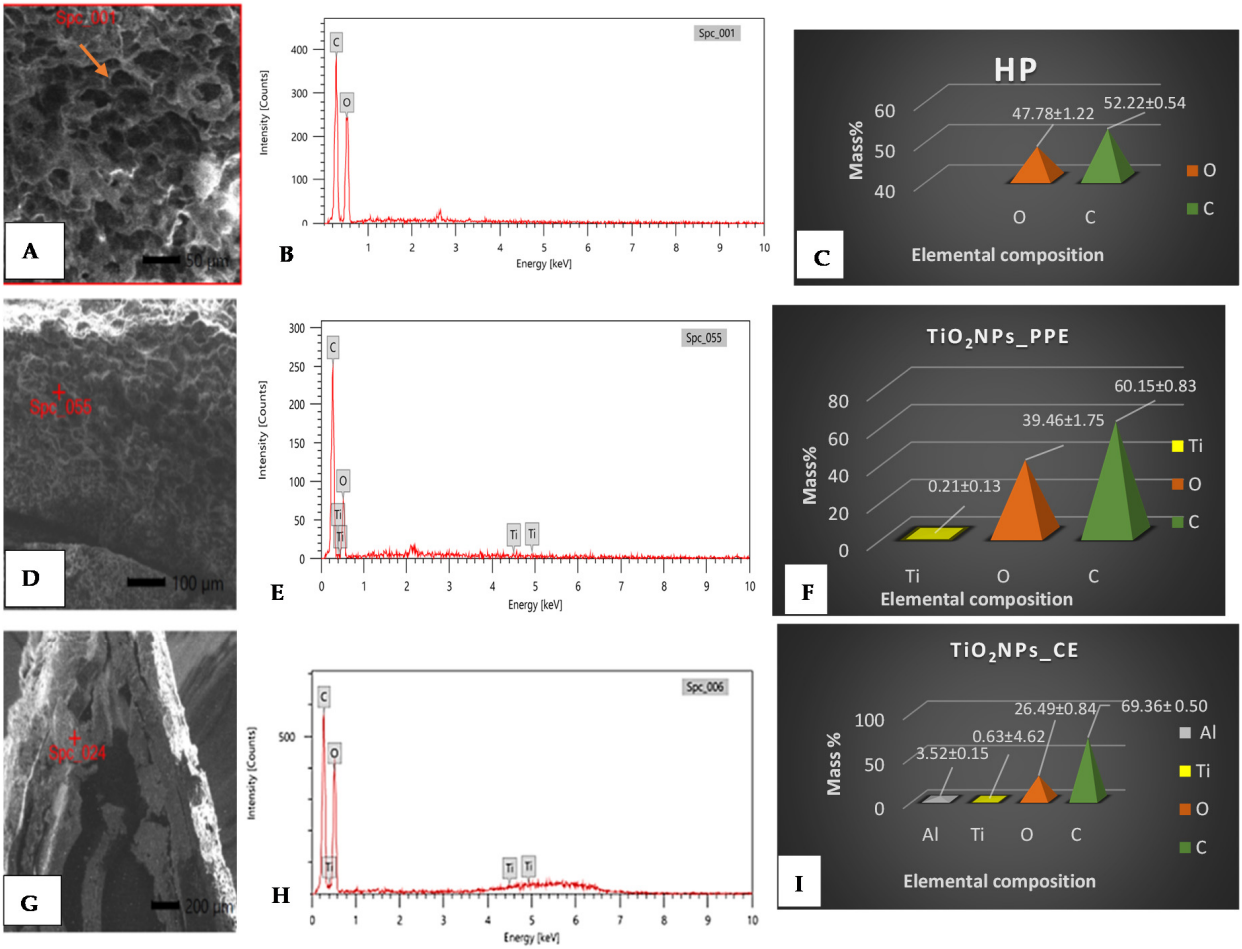


Figure 5. SEM–EDX-based analysis of hydroprimed seeds of *P. granatum* (**A**–**C**). Panels (**D**–**F**) show the adsorption of TiO_2NPs_PPE and (**G**,**H**) show the adsorption of TiO_2NPs_CE, and their detection by EDX on the surface of the seed coat. EDX spectra show element (C, O, and Ti) peaks and mass percentage of them. The SEM images represent the seed surface's region of interest (ROI). The amount of the adsorbed C, O and Ti elements (**C**,**F**,**I**) is expressed as mean values of mass % obtained from sample replicates used for investigation, i.e., mean (%) ± SE.

3.3. TiO_2NP Uptake in Seeds

3.3.1. TEM Analysis

The translocation of TiO_2NPs across the seed coat into the seed embryos of *P. granatum* was examined by means of TEM, in which TiO_2NPs were observed as dark particles and aggregates within the cell vacuoles. Obviously, the TEM micrographs confirmed the presence of TiO_2NPs inside the seed embryos as scattered deposits of tetragonal and cylindrical crystals (Figure 6B,C). They are typically compatible with TEM images of biosynthesized TiO_2NPs. On the other hand, no NPs were detected in the control, hydroprimed seeds (Figure 6A).

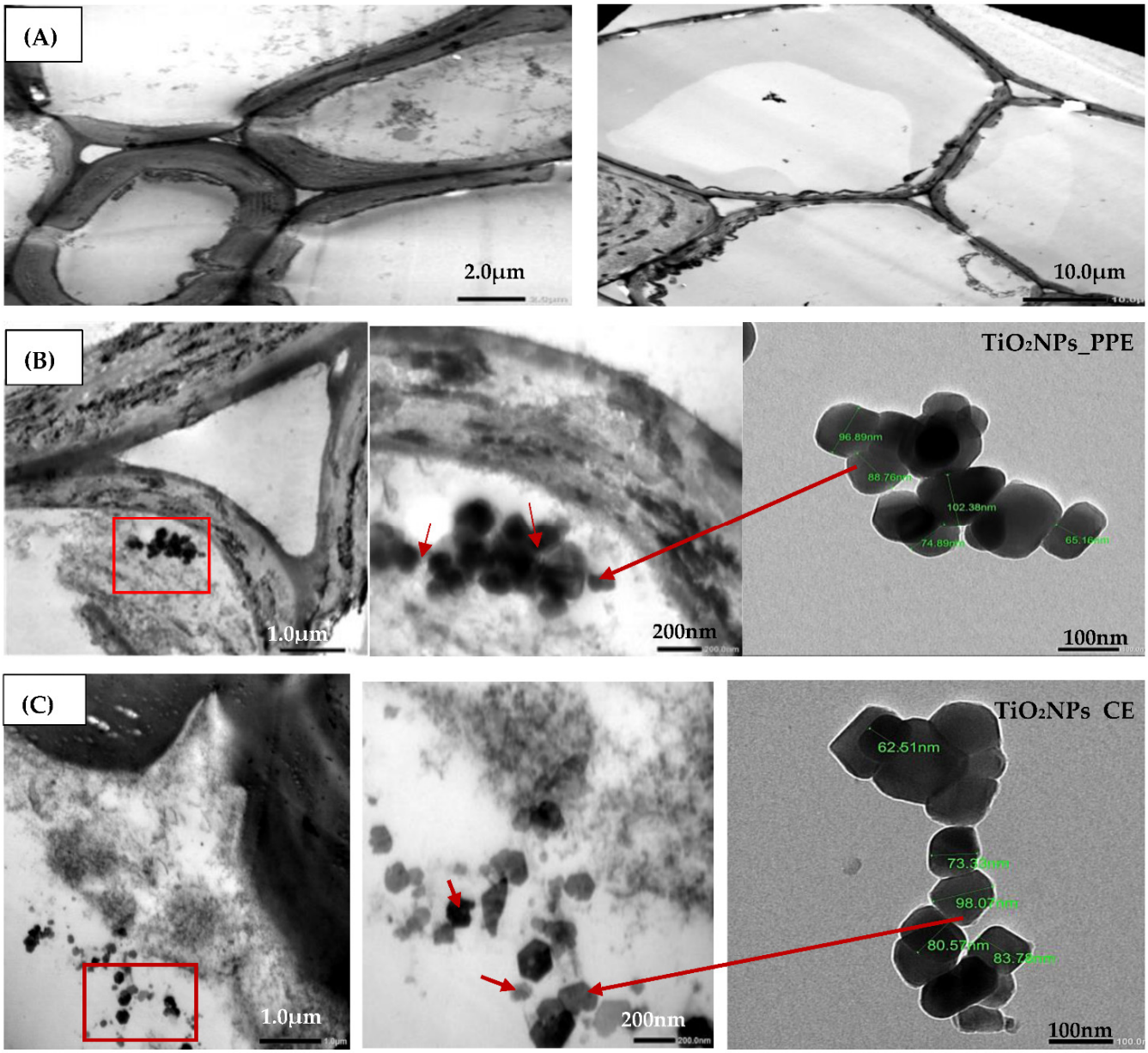
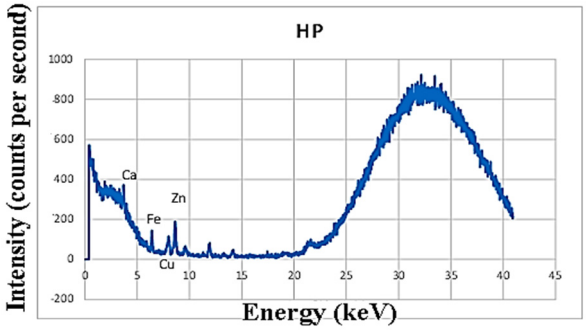


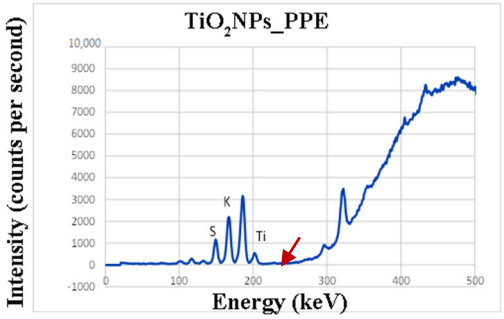
Figure 6. TEM images of seeds of P. granatum treated with 40 mg/L TiO_2NPs suspension for 24 h., demonstrating cross-sections of seeds after priming by: (**A**) distilled water (hydroprimed), (**B**) TiO_2NPs_PPE and (**C**) TiO_2NPs_CE. Details of the clusters constituted by Ti dioxide nanoparticles inside seed tissue are in the same pattern as revealed by the TEM image of synthesized NPs. (Red boxes and arrows indicate the detected TiO_2NPs).

3.3.2. X-ray Fluorescence (XRF) and ICP–OES Analyses

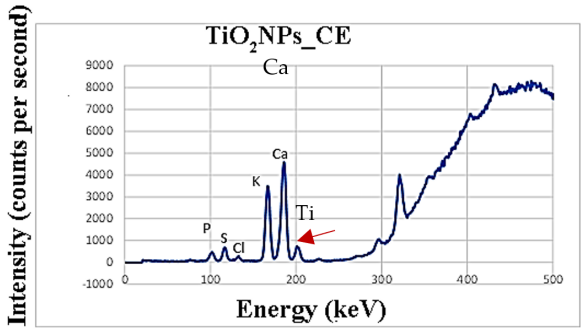
To monitor the uptake of metal oxide nanoparticles, the TEM images only reveal the particle size and surface morphology of the sample. Therefore, in the present research, XRF and ICP–OES analyses were undertaken for the quantitative measurement of TiO_2NPs incorporating primed seeds. Both methods confirmed the assimilation of TiO_2NPs by nanoprimed seeds at a concentration of 40 mg/L. The XRF spectral analysis showed Ti peaks in both the TiO_2NPs_PPE and TiO_2NPs_CE samples (Figure 7B,C) compared to the hydroprimed samples (Figure 7A). A comparison of the results obtained from the analysis of the fine-powdered nanoprimed seed samples by ICP–OES and XRF is presented in Figure 8. There were evident variations between the ICP–OES and XRF analyses. In the case of TiO_2NPs_CE, the Ti content was 7.3 times (0.022 mg/g) higher for XRF than for ICP–OES (0.003 mg/g) at 40 mg/L. XRF was unable to detect it in TiO_2NPs_PPE, suggesting that the content in those samples was below the detection limit (BDL) of this technique. Conversely, the amount of Ti detected by ICP–OES was 0.013 mg/g in the same treatment.



(**A**)



(**B**)



(**C**)

Figure 7. Analysis of *P. granatum* L. seeds treated with TiO_2NPs using X-ray fluorescence spectroscopy (XRF), compared with hydroprimed seeds. (**A**): Hydroprimed seeds (HP); (**B**): seeds primed by TiO_2NPs_PPE; (**C**): seeds primed by TiO_2NPs_CE. Arrows indicate Ti signal in nanoprimed seeds.

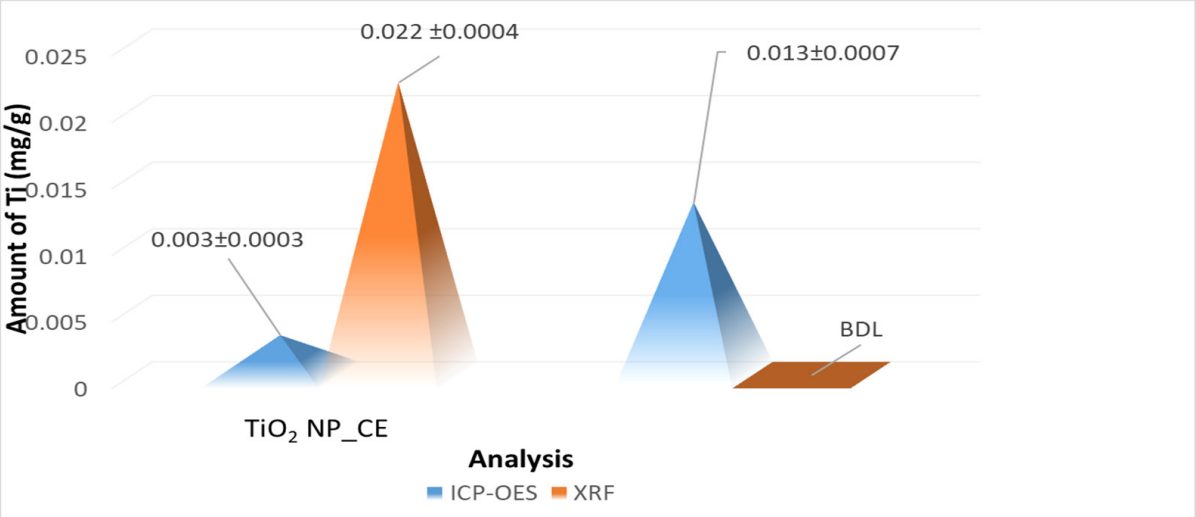


Figure 8. XRF and ICP–OES measurements of TiO_2NPs (mg/g) in *P. granatum* seeds exposed to TiO_2NPs_PPE and TiO_2NPs_CE. The amount of Ti element is expressed as mean values obtained from sample replicates used for investigation, i.e., mean ± SE.

4. Discussion

The bioproduction of nanoparticles is an innovative cost-effective and low-risk technique to synthesize nanoparticles [26]. In this study, titanium dioxide nanoparticles (TiO_2NPs) were successfully synthesized using an aqueous extract of pomegranate peel and coffee residue as a reducing and stabilizing agent source, and the pure anatase form of titanium dioxide was confirmed by different characterization techniques. The color change noticed during the synthesis of TiO_2NPs has been reported for similar studies when extracts from diverse types of plant parts were used [27,28]. The change in color is attributed to the gradual reduction of Ti^{+2} to Ti^0 [27].

The recorded UV–V is spectrum showed a maximum absorbance near the range of 320 nm and 350 nm, proving the reduction of titanium ions to colloidal titanium. Other reports have revealed different absorption spectra of green-synthesized TiO_2NPs using *Echinacea purpurea herba*, *Hibiscus* flower, and *Aloe vera* extracts in the range of 200 and 400 nm [29]. The obtained absorption spectrum of the produced TiO_2NPs is affected by the particle size, shape, and agglomeration. However, the UV–Vis results verified the anatase phase of the formed TiO_2NPs as they absorb light within the range of 320–350 nm. It has been suggested that anatase particles absorb light at wavelengths lower than 385 nm, while rutile-phase particles absorb light at higher wavelengths [30].

Higher zeta potential negativity (−15.0 mV) has been reported as a key reason for small-scale TiO_2NPs because of the increasing electrostatic repulsive forces between the nanoparticle surfaces that prevent their aggregation to larger particles [31]. Based on our current findings, which revealed that the green-synthesized TiO_2NPs using CE displayed smaller sizes and a greater zeta potential negativity than those synthesized from PPE, the formation of higher clusters could be observed in TiO_2NPs_PPE (439.6 nm by DLS, 85.6 nm by TEM) on the surface of the seeds, whereas the TiO_2NPs_CE (45.14 nm by DSL, 79.6 nm by TEM) showed individual nanoparticles and some clusters. In the same context, Al Qarni et al. [32] succeeded in synthesizing nanoporous anatase-phase TiO_2 using coffee husk extract with a small-scale size of 7.5 nm, whereas Abu-Dalo et al. [31] synthesized TiO_2NPs using PPE with a Z-average size of 620 nm and zeta potential of 6.95 mV. XRD data also confirmed that crystalline TiO_2NPs exhibited a strong anatase phase with 2θ values of 25.28° and 48.37°, and the small size was proven by broad peaks [33], which concur with the JCPDS file No. 21-1272 [34].

Studies on the FTIR of green-synthesized NPs are crucial for understanding phytoconstituent behavior in the process of nanoparticle synthesis [35]. Here, the FTIR spectra

indicated that the biomolecules of pomegranate (PPE) and coffee (CE), such as alkaloids, coumarins, flavonoids, tannins, and terpenoids, were effective in synthesizing TiO_2NPs through Ti–O-Ti capping [36–38]. These biomolecules are responsible for the reduction of bulk titanium dioxide to stable TiO_2 [39]. The higher number of sharp peaks and broad bands in the TiO_2NPs_CE spectra could be attributed to the presence of free caffeine in addition to those that refer to flavonoids as in TiO_2NPs_PPE. The recorded vibrations of caffeine in this study are in accordance with previous reports [32,40]. These bioactive molecules function as templates during the synthesis process to maintain phase stability and prevent the overgrowth and aggregation of TiO_2NPs.

Understanding the uptake and incorporation of NPs into seeds in response to nanopriming techniques is challenging because qualitative and quantitative methods are still being developed and the comparability of results among different methods is unclear [18]. In this study, the uptake of TiO_2NPs at 40 mg/L by nanoprimed pomegranate (*P. granatum* L.) seeds was evaluated using different analytical techniques. The SEM micrographs of the seeds elucidated that the nanopriming process is highly effective in creating well-developed pores on the seed surface of *P. granatum* L., leading to a large surface area and porous structure of the seed coat [41]. These pores offered an appropriate surface for mineral compounds to be captured and adsorbed on the seed coat. By assessing the properties of both NPs (TiO_2NPs_PPE and TiO_2NPs_CE), it could be concluded that a variable capacity for pore formation can be found in relation to the size, shape, and functional groups covered on the surface, which greatly influence the creation of seed coat nanopores [41]. Smaller nanoparticles are generally considered to have a higher surface energy; therefore, they may interact with the cell wall, causing the expansion of existing pores or the development of new pores; therefore, NPs that penetrate seed coats and create small pores may lead to increased NPs incorporation [42]. Likewise, the XRF analysis confirmed a higher amount of TiO_2NPs_CE inside the seeds than TiO_2NPs_PPE. There is a possibility that nanoparticles of small size could pass through pores and reach the plasma membrane. Additionally, they may enlarge existing pores or contribute to the formation of new pores in the cell wall [43–45]. Considering its smaller size and higher zeta potential, TiO_2NPs_CE could be considered as a more effective NP for creating well-defined pores in seed coats. The mechanisms of NP penetration into cells should be understood in the context of the parameters related to the NP movement. Therefore, additional investigations are necessary to examine those mechanisms comprehensively.

The efficiency of adsorbing NPs has been attributed to the higher amount of carbon compared to oxygen [45]. Based on an EDX analysis of the studied nanoprimed seeds, the coffee extract has been validated as having greater capping, reducing, and adsorption capacities than pomegranate extract. The physical adsorption of TiO_2NPs on specific regions of the seed is associated with the formation of distinct shapes and clustering of agglomerates [46,47]. The accumulation on the seed surface could be attributed to mechanical adhesion or diffusion, as previously observed with other metal oxide nanoparticles, e.g., ZnO, CeO_2, or CuO [48–50]. The generated EDX analysis of the elementary composition coincides with the FTIR spectrum, which revealed a higher number of sharp peaks and broad bands of TiO_2NPs_CE compared to TiO_2NPs_PPE. This could be attributed to the C=O stretching vibration of the carbonyl group and the C=C aromatic stretching vibration [51]. Therefore, the seeds primed with TiO_2NPs_CE revealed an enhanced carbon (C) signal due to the imidazole ring of the caffeine polymer in addition to the more activated carbons derived during the processing of the coffee ground and the preparation of CE. The typical moieties present in the coffee ground were also identified in other studies [52,53], e.g., the aliphatic C-H stretching vibration.

The incorporation of TiO_2NPs into the pomegranate seeds was revealed by TEM, XRF and ICP–OES with Ti detection. The results demonstrated that pomegranate seeds do not contain naturally occurring Ti, but they incorporate TiO_2NPs when primed with them. In TEM images, TiO_2NPs were observed as dark, electron-dense deposits within the cytoplasm of the treated seeds, which was identified as elemental Ti by XRF analysis.

The distribution of intracellular TiO_2NPs showed no clear pattern and tended to appear as clusters close to the plasma membranes. These TiO_2NPs clusters may arise from the agglomeration of internalized individual particles under the dynamic cytoplasmic physiological environment [22]. The TEM results are in agreement with recent studies showing the internalization and uptake of NPs in the seeds of other plant species (e.g., watermelon [2], corn [47], rice [18] and tomato [22]).

While the EM analysis provides definitive detection and distribution patterns of NPs in plant tissues, only a small fraction of the plant area can be analyzed using this technique [18]. Elemental analysis using XRF provided complementary information considering that the synthesized TiO_2NPs could be easily quantified and compared to the concentration measured by ICP–OES. Despite the differences in TiO_2 content between samples taken for the XRF and ICP–OES analyses, both methods were able to confirm that TiO_2NPs can penetrate through seed coats and interact with seeds. Discrepancies between XRF and ICP–OES values have also been reported by other researchers [54,55]. The content of TiO_2NPs_CE determined by XRF was higher than the values determined by ICP–OES; this is perhaps due to the fact that XRF is a non-destructive method that allows the direct measurement and avoids the loss associated with sample pre-treatment, thus avoiding leakages. In contrast, XRF sensitivity tends to rapidly decrease with particle size, and since TiO_2NPs_PPE are larger than TiO_2NPs_CE, seeds may only be able to uptake a limited amount due to NPs aggregating below the XRF detection limit; this could explain the higher TiO_2NPs_PPE content found by ICP–OES.

In agreement with those results obtained from exposed Mung beans [29] and maize seeds [56], TiO_2NPs were able to penetrate pomegranate seeds, as confirmed through TEM, XRF, and ICP–OES, which is the first direct evidence of TiO_2NP uptake in pomegranate seed tissues. Such evidence of TiO_2 internalization by plant tissues is also in accordance with a variety of other metal-based nanoparticles, including Fe_3O_4, Au, and Cu nanoparticles [57–59].

5. Conclusions

Our research undertook nanoparticle-mediated seed-priming treatment aimed at reducing the release of substantial amounts of nanomaterials into the field and lowering impacts on the environment. The main study findings can be summarized as follows:

1. TiO_2 nanoparticles from aqueous extracts of pomegranate fruit peel (PPE) and coffee (CE) were successfully synthesized using the green synthesis method in pure anatase form.
2. The evaluation of the uptake and internalization by seeds via different analytical techniques showed that nanopriming with TiO_2NPs had positive efficacy on the uptake and incorporation by pomegranate (*P. granatum* L.) seeds.
3. The EM analysis offered definitive determination of the NPs in the plant tissues and information about the distribution of the NPs within the tissues. The total elemental analysis using EDX, XRF, and ICP–OES also provided complementary information to the SEM/TEM, reflecting the significance of an integrative approach for verifying the incorporation of nanoparticles inside seed tissues.

However, there is a need for the administration of a safe dose of nanoparticles in the environment and toxicity-focused research. Thus, the further strengthening of nanopriming effectiveness treatments is needed through the optimization of experimental conditions. Additionally, it is imperative to study different plant species, as the results observed in one crop are not necessarily applicable to the other crops. As part of our current and future research, we will focus on the molecular mechanisms involved in plant response to nanopriming applications, including germination and growth experiments, as well as physiology, metabolism, and genetics, which will contribute to the sustainable development of agriculture in the Taif region and improve the socioeconomic status of farmers.

Author Contributions: Conceptualization, H.M.A.; Data curation, M.M.M. and N.A.H.; Formal analysis, H.M.A. and M.M.M.; Funding acquisition, H.M.A.; Investigation, M.M.M., N.A.H. and A.A.A.; Methodology, H.M.A., M.M.M., N.A.H., A.A.A. and A.A.; Project administration, H.M.A.; Resources, H.M.A.; Software, N.A.H.; Supervision, H.M.A.; Visualization, N.A.H.; Writing—original draft, H.M.A., M.M.M., N.A.H., A.A.A. and A.A.; Writing—review and editing, H.M.A., N.A.H. All authors have read and agreed to the published version of the manuscript.

Funding: This work was financially supported by a research project No. [1-441-130] from the Ministry of Education in Saudi Arabia.

Acknowledgments: The authors extend their appreciation to the Deputyship for research and innovation, Ministry of Education in Saudi Arabia, for funding this research work through project number 1-441-130.

Conflicts of Interest: No conflict of interest.

References

1. Chen, K.; Arora, R. Priming memory invokes seed stress-tolerance. *Environ. Exp. Bot.* **2013**, *94*, 33–45. [CrossRef]
2. Acharya, P.; Jayaprakasha, G.K.; Crosby, K.M.; Jifon, J.L.; Patil, B.S. Nanoparticle-mediated seed priming improves germination, growth, yield, and quality of watermelons (*Citrullus lanatus*) at multilocations in Texas. *Sci. Rep.* **2020**, *10*, 5037. [CrossRef]
3. Sarikhani, H.; Valipour, M.; Chehregani, A. Fruit growth and patterns of lignification in the seeds of four Iranian pomegranate (*Punica granatum* L.) cultivars. *J. Hortic. Sci. Biotechnol.* **2014**, *89*, 268–272. [CrossRef]
4. Phat, P.; Sheikh, S.; Lim, J.H.; Kim, T.B.; Seong, M.H.; Chon, H.G.; Shin, Y.K.; Song, Y.J.; Noh, J. Enhancement of Seed Germination and Uniformity in Triploid Watermelon (*Citrullus lanatus* (Thunb.) Matsum. and Nakai). *Korean J. Hortic. Sci. Technol.* **2015**, *33*, 932–940. [CrossRef]
5. El-Sanatawy, A.M.; Ash-Shormillesy, S.M.A.I.; Qabil, N.; Awad, M.F.; Mansour, E. Seed Halo-Priming Improves Seedling Vigor, Grain Yield, and Water Use Efficiency of Maize under Varying Irrigation Regimes. *Water* **2021**, *13*, 2115. [CrossRef]
6. Shah, T.; Latif, S.; Khan, H.; Munsif, F.; Nie, L. Ascorbic Acid Priming Enhances Seed Germination and Seedling Growth of Winter Wheat under Low Temperature Due to Late Sowing in Pakistan. *Agronomy* **2019**, *9*, 757. [CrossRef]
7. Song, K.; He, X. How to improve seed germination with green nanopriming. *Seed Sci. Technol.* **2021**, *49*, 81–92. [CrossRef]
8. Khalaki, M.A.; Moameri, M.; Lajayer, B.A.; Astatkie, T. Influence of nano-priming on seed germination and plant growth of forage and medicinal plants. *Plant Growth Regul.* **2021**, *93*, 13–28. [CrossRef]
9. Shang, Y.; Hasan, M.K.; Ahammed, G.J.; Li, M.; Yin, H.; Zhou, J. Applications of Nanotechnology in Plant Growth and Crop Protection: A Review. *Molecules* **2019**, *24*, 2558. [CrossRef]
10. Malik, A.; Mor, V.S.; Tokas, J.; Punia, H.; Malik, S.; Malik, K.; Sangwan, S.; Tomar, S.; Singh, P.; Singh, N.; et al. Biostimulant-Treated Seedlings under Sustainable Agriculture: A Global Perspective Facing Climate Change. *Agronomy* **2021**, *11*, 14. [CrossRef]
11. Mahakham, W.; Sarmah, A.K.; Maensiri, S.; Theerakulpisut, P. Nanopriming technology for enhancing germination and starch metabolism of aged rice seeds using phytosynthesized silver nanoparticles. *Sci. Rep.* **2017**, *7*, 8263. [CrossRef]
12. Spielman-Sun, E.; Avellan, A.; Bland, G.D.; Tappero, R.V.; Acerbo, A.S.; Unrine, J.M.; Giraldo, J.P.; Lowry, G.V. Nanoparticle surface charge influences translocation and leaf distribution in vascular plants with contrasting anatomy. *Environ. Sci. Nano* **2019**, *6*, 2508–2519. [CrossRef]
13. An, J.; Hu, P.; Li, F.; Wu, H.; Shen, Y.; White, J.C.; Tian, X.; Li, Z.; Giraldo, J.P. Emerging investigator series: Molecular mechanisms of plant sa-linity stress tolerance improvement by seed priming with cerium oxide nanoparticles. *Environ. Sci. Nano* **2020**, *7*, 2214–2228. [CrossRef]
14. Singh, P.; Kim, Y.J.; Zhang, D.; Yang, D.C. Biological Synthesis of Nanoparticles from Plants and Microorganisms. *Trends Biotechnol.* **2016**, *34*, 588–599. [CrossRef]
15. Rajan, R.; Chandran, K.; Harper, S.L.; Yun, S.I.; Kalaichelvan, P.T. Plant extract synthesized silver nanoparticles: An ongoing source of novel biocompatible materials. *Ind. Crop. Prod.* **2015**, *70*, 356–373. [CrossRef]
16. Khan, M.; Shaik, M.R.; Adil, S.F.; Khan, S.T.; Al-Warthan, A.; Siddiqui, M.R.H.; Tahir, M.N.; Tremel, W. Plant extracts as green reductants for the synthesis of silver nanoparticles: Lessons from chemical synthesis. *Dalton Trans.* **2018**, *47*, 11988–12010. [CrossRef]
17. Abdelmigid, H.M.; Morsi, M.M.; Hussien, N.A.; Alyamani, A.A.; Al Sufyani, N.M. Comparative Analysis of Nanosilver Particles Synthesized by Different Approaches and Their Antimicrobial Efficacy. *J. Nanomater.* **2021**, *2021*, 2204776. [CrossRef]
18. Deng, Y.; Petersen, E.J.; Challis, K.E.; Rabb, S.A.; Holbrook, R.D.; Ranville, J.F.; Nelson, B.C.; Xing, B. Multiple method analysis of TiO_2 nanoparticle uptake in rice (*Oryza sativa* L.) plants. *Environ. Sci. Technol.* **2017**, *51*, 10615–10623. [CrossRef]
19. Kumari, M.; Ernest, V.; Mukherjee, A.; Chandrasekaran, N. In Vivo Nanotoxicity Assays in Plant Models. *Methods Mol. Biol.* **2012**, *926*, 399–410. [CrossRef]
20. Pérez-de-Luque, A. Interaction of Nanomaterials with Plants: What Do We Need for Real Applications in Agriculture? *Front. Environ. Sci.* **2017**, *5*, 12. [CrossRef]

21. Lv, J.; Christie, P.; Zhang, S. Uptake, translocation, and transformation of metal-based nanoparticles in plants: Recent advances and methodological challenges. *Environ. Sci. Nano* **2019**, *6*, 41–59. [CrossRef]
22. Nicolás-Álvarez, D.E.; Andraca-Adame, J.A.; Chanona-Pérez, J.J.; Méndez-Méndez, J.V.; Borja-Urby, R.; Cayetano-Castro, N.; Martínez-Gutiérrez, H.; López-Salazar, P. Effects of TiO_2 Nanoparticles Incorporation into Cells of Tomato Roots. *Nanomaterials* **2021**, *11*, 1127. [CrossRef]
23. Swathi, N.; Sandhiya, D.; Rajeshkumar, S.; Lakshmi, T. Green synthesis of titanium dioxide nanoparticles using Cassia fistula and its antibacterial activity. *Int. J. Res. Pharm. Sci.* **2019**, *10*, 856–860. [CrossRef]
24. Ahmad, W.; Jaiswal, K.K.; Soni, S. Green synthesis of titanium dioxide (TiO_2) nanoparticles by using *Mentha arvensis* leaves extract and its antimicrobial properties. *Inorg. Nano Metal Chem.* **2020**, *50*, 1032–1038. [CrossRef]
25. Tezotto, T.; Favarin, J.L.; Neto, A.P.; Gratão, P.L.; Azevedo, R.A.; Mazzafera, P. Simple procedure for nutrient analysis of coffee plant with energy dispersive X-ray fluorescence spectrometry (EDXRF). *Sci. Agric.* **2013**, *70*, 263–267. [CrossRef]
26. Baghaienezhad, M.; Boroghani, M.; Anabestani, R. Silver nanoparticles Synthesis by coffee residues extract and their antibacterial activity. *Nanomed. Res. J.* **2020**, *5*, 29–34.
27. Mathew, S.S.; Sunny, N.E.; Shanmugam, V. Green synthesis of anatase titanium dioxide nanoparticles using Cuminum cyminum seed extract; effect on Mung bean (*Vigna radiata*) seed germination. *Inorg. Chem. Commun.* **2021**, *126*, 108485. [CrossRef]
28. Aravind, M.; Amalanathan, M.; Mary, M.S.M. Synthesis of TiO_2 nanoparticles by chemical and green synthesis methods and their multifaceted properties. *SN Appl. Sci.* **2021**, *3*, 409. [CrossRef]
29. Bekele, E.T.; Gonfa, B.A.; Sabir, F.K. Use of Different Natural Products to Control Growth of Titanium Oxide Nanoparticles in Green Solvent Emulsion, Characterization, and Their Photocatalytic Application. *Bioinorg. Chem. Appl.* **2021**, *2021*, 6626313. [CrossRef]
30. Waleczek, M.; Dendooven, J.; Dyachenko, P.; Petrov, A.Y.; Eich, M.; Blick, R.H.; Detavernier, C.; Nielsch, K.; Furlan, K.P.; Zierold, R. Influence of Alumina Addition on the Optical Properties and the Thermal Stability of Titania Thin Films and Inverse Opals Produced by Atomic Layer Deposition. *Nanomaterials* **2021**, *11*, 1053. [CrossRef]
31. Abu-Dalo, M.; Jaradat, A.; Albiss, B.A.; Al-Rawashdeh, N.A.F. Green synthesis of TiO_2 NPs/pristine pomegranate peel extract nanocomposite and its antimicrobial activity for water disinfection. *J. Environ. Chem. Eng.* **2019**, *7*, 103370. [CrossRef]
32. Al Qarni, F.; Alomair, N.A.; Mohamed, H.H. Environment-Friendly Nanoporous Titanium Dioxide with Enhanced Photocatalytic Activity. *Catalysts* **2019**, *9*, 799. [CrossRef]
33. Prabhu, C.A.; Silambarasan, D.; Sarika, R.; Selvam, V. Synthesis and characterization of TiO_2. *Mater. Today Proc.* **2022**. [CrossRef]
34. Sutradhar, P.; Saha, M.; Maiti, D. Microwave synthesis of copper oxide nanoparticles using tea leaf and coffee powder extracts and its antibacterial activity. *J. Nanostruct. Chem.* **2014**, *4*, 86. [CrossRef]
35. Aisida, S.O.; Madubuonu, N.; Alnasir, M.H.; Ahmad, I.; Botha, S.; Maaza, M.; Ezema, F.I. Biogenic synthesis of iron oxide nanorods using Moringa oleifera leaf extract for antibacterial applications. *Appl. Nanosci.* **2020**, *10*, 305–315. [CrossRef]
36. León, A.; Reuquen, P.; Garín, C.; Segura, R.; Vargas, P.; Zapata, P.; Orihuela, P.A. FTIR and Raman Characterization of TiO_2 Nanoparticles Coated with Polyethylene Glycol as Carrier for 2-Methoxyestradiol. *Appl. Sci.* **2017**, *7*, 49. [CrossRef]
37. Bagheri, S.; Shameli, K.; Abd Hamid, S.B. Synthesis and Characterization of Anatase Titanium Dioxide Nanoparticles Using Egg White Solution via Sol-Gel Method. *J. Chem.* **2013**, *2013*, 848205. [CrossRef]
38. Mayedwa, N.; Mongwaketsi, N.; Khamlich, S.; Kaviyarasu, K.; Matinise, N.; Maaza, M. Green synthesis of nickel oxide, palladium and palladium oxide synthesized via Aspalathus linearis natural extracts: Physical properties & mechanism of formation. *Appl. Surf. Sci.* **2018**, *446*, 266–272. [CrossRef]
39. Sundrarajan, M.; Bama, K.; Bhavani, M.; Jegatheeswaran, S.; Ambika, S.; Sangili, A.; Nithya, P.; Sumathi, R. Obtaining titanium dioxide nanoparticles with spherical shape and antimicrobial properties using M. citrifolia leaves extract by hydrothermal method. *J. Photochem. Photobiol.* **2017**, *171*, 117–124.
40. Srivastava, S.K.; Singh, V.B. Ab initio and DFT studies of the structure and vibrational spectra of anhydrous caffeine. *Spectrochim. Acta Part A Mol. Biomol. Spectrosc.* **2013**, *115*, 45–50. [CrossRef]
41. Bello, O.S.; Adegoke, K.A.; Akinyunni, O.O. Preparation and characterization of a novel adsorbent from Moringa oleifera leaf. *Appl. Water Sci.* **2017**, *7*, 1295–1305. [CrossRef]
42. Tang, Y.J.; Wu, S.G.; Huang, L.; Head, J.; Chen, D.R.; Kong, I.C. Phytotoxicity of Metal Oxide Nanoparticles is Related to Both Dissolved Metals Ions and Adsorption of Particles on Seed Surfaces. *J. Pet. Environ. Biotechnol.* **2012**, *3*, 126. [CrossRef]
43. Kurczyńska, E.; Godel-Jędrychowska, K.; Sala, K.; Milewska-Hendel, A. Nanoparticles—Plant Interaction: What We Know, Where We Are? *Appl. Sci.* **2021**, *11*, 5473. [CrossRef]
44. Xu, L.; Zhu, Z.; Sun, D.W. Bioinspired Nanomodification Strategies: Moving from Chemical-Based Agrosystems to Sustainable Agriculture. *ACS Nano* **2021**, *15*, 12655–12686. [CrossRef]
45. Xiong, C.; Zheng, Y.; Feng, Y.; Yao, C.; Ma, C.; Zheng, X.; Jiangd, J. Preparation of a novel chloromethylated polystyrene-2-amino-1,3,4-thiadiazole chelating resin and its adsorption properties and mechanism for separation and recovery of Pt (IV) from aqueous solutions. *J. Mater. Chem. A* **2014**, *2*, 5379–5386. [CrossRef]
46. Khan, Z.S.; Rizwan, M.; Hafeez, M.; Ali, S.; Javed, M.R.; Adrees, M. The accumulation of cadmium in wheat (*Triticum aestivum*) as influenced by zinc oxide nanoparticles and soil moisture conditions. *Environ. Sci. Pollut. Res. Int.* **2019**, *26*, 19859–19870. [CrossRef]

47. Segatto, C.; Ternus, R.; Junges, M.; de Mello, J.M.M.; da Luz, G.L.; Riella, H.G.; Silva, L.L.; Lajús, C.R.; Fiori, M.A. Adsorption and incorporation of the zinc oxide nanoparticles in seeds of corn: Germination performance and antimicrobial protection. *Int. J. Adv. Eng. Res. Sci.* **2018**, *5*, 2456–6495. [CrossRef]
48. Kong, I.C.; Ko, K.-S.; Koh, D.-C. Comparisons of the Effect of Different Metal Oxide Nanoparticles on the Root and Shoot Growth under Shaking and Non-Shaking Incubation, Different Plants, and Binary Mixture Conditions. *Nanomaterials* **2021**, *11*, 1653. [CrossRef]
49. Zhao, L.J.; Peralta-Videa, J.R.; Ren, M.; Varela-Ramirez, A.; Li, C.; Hernandez-Viezcas, J.A.; Aguilera, R.J.; Gardea-Torresdey, J.L. Transport of Zn in a sandy loam soil treated with ZnO NPs and uptake by corn plants: Electron microprobe and confocal microscopy studies. *Chem. Eng. J.* **2012**, *184*, 1–8. [CrossRef]
50. Deng, Y.Q.; White, J.C.; Xing, B.S. Interactions between engineered nanomaterials and agricultural crops: Implications for food safety. *J. Zhejiang Univ. Sci.* **2014**, *15*, 552–572. [CrossRef]
51. Corral-Bobadilla, M.; Lostado-Lorza, R.; Somovilla-Gómez, F.; Escribano-García, R. Effective use of activated carbon from olive stone waste in the biosorption removal of Fe(III) ions from aqueous solutions. *Clean. Prod.* **2021**, *294*, 126332. [CrossRef]
52. El-Azazy, M.; El-Shafie, A.S.; Morsy, H. Biochar of Spent Coffee Grounds as Per Se and Impregnated with TiO_2: Promising Waste-Derived Adsorbents for Balofloxacin. *Molecules* **2021**, *26*, 2295. [CrossRef] [PubMed]
53. Rosson, E.; Garbo, F.; Marangoni, G.; Bertani, R.; Lavagnolo, M.C.; Moretti, E.; Talon, A.; Mozzon, M.; Sgarbossa, P. Activated Carbon from Spent Coffee Grounds: A Good Competitor of Commercial Carbons for Water Decontamination. *Appl. Sci.* **2020**, *10*, 5598. [CrossRef]
54. Arenas, L.; Ortega, M.; García-Martínez, M.J.; Querol, E.; Llamas, J.F. Geochemical characterization of the mining district of Linares (Jaen, Spain) by means of XRF and ICP-AES. *J. Geochem. Explor.* **2011**, *108*, 21–26. [CrossRef]
55. Chojnacka, K.; Samoraj, M.; Tuhy, Ł.; Michalak, I.; Mironiuk, M.; Mikulewicz, M. Using XRF and ICP-OES in Biosorption Studies. *Molecules* **2018**, *23*, 2076. [CrossRef]
56. Shah, T.; Latif, S.; Saeed, F.; Ali, I.; Ullah, S.; Alsahli, A.; Jan, S.; Ahmad, P. Seed priming with titanium dioxide nanoparticles enhances seed vigor, leaf water status, and antioxidant enzyme activities in maize (*Zea mays* L.) under salinity stress. *J. King Saud Univ. Sci.* **2021**, *33*, 101207. [CrossRef]
57. Tombuloglu, H.; Slimani, Y.; Tombuloglu, G.; Korkmaz, A.D.; Baykal, A.; Almessiere, M.; Ercan, I. Impact of superparamagnetic iron oxide nanoparticles (SPIONs) and ionic iron on physiology of summer squash (*Cucurbita pepo*): A comparative study. *Plant Physiol. Biochem.* **2019**, *139*, 56–65. [CrossRef]
58. Judy, J.D.; Unrine, J.M.; Rao, W.; Wirick, S.; Bertsch, P.M. Bioavailability of Gold Nanomaterials to Plants: Importance of Particle Size and Surface Coating. *Environ. Sci. Technol.* **2012**, *46*, 8467–8474. [CrossRef]
59. Ibrahim, A.S.; Ali, G.A.M.; Hassanein, A.; Attia, A.M.; Marzouk, E.R. Toxicity and Uptake of CuO Nanoparticles: Evaluation of an Emerging Nanofertilizer on Wheat (*Triticum aestivum* L.) Plant. *Sustainability* **2022**, *14*, 4914. [CrossRef]